STIC-ILL

105/2

393859

From: Baskar, Padmavathi
Sent: Thursday, May 02, 2002 8:10 AM
To: STIC-ILL
Subject: 08913811

COULD YOU PLEASE GET THESE REFERENCES AS AN URGENT ORDER. THANKS FOR ALL THE HELP.

Gross et al. (J. of Neuroscience Methods 5: 13-22, 1982) 7057675

Ambros-Ingerson et al (Brain Research (1993) 620:237-244).

Padma Baskar
Art Unit 1645
Patent Examiner/Biotechnology
CM-1, 8E-13, BOX 8E-12
703-308-8886

6785957

Unable to
Elec
Conv

Journal of Neuroscience Methods, 5 (1982) 13–22
Elsevier Biomedical Press.

Recording of spontaneous activity with photoetched microelectrode surfaces from mouse spinal neurons in culture

Guenter W. Gross, Ann N. Williams and Jen H. Lucas

Department of Biology, The Texas Woman's University, Denton, TX 76204 (U.S.A.)

(Received April 7th, 1981)
(Revised version received July 20th, 1981)
(Accepted July 27th, 1981)

Key words: photoetched electrodes — cell culture — laser deinsulation — mouse spinal neurons — multielectrode surface

A matrix of photoetched gold conductors integrated into the floor of a tissue culture chamber has been used to record from mammalian spinal cord neurons grown on the insulation layer of the multielectrode plate. Spontaneous activity has been monitored from tissue microfragments less than 150 μm in diameter and from thin sheets of spinal cell aggregates. Maximum spike amplitudes of 360 μV with signal-to-noise ratios of 8 : 1 have so far been achieved and the spontaneous activity maintained for several days. Recording electrode impedances measured between 4 and 7 MΩ at 1 kHz. Conductor tips were deinsulated with laser pulses that formed shallow craters 2 μm deep and 12 μm in diameter. Addition of colloidal gold or platimum black was not necessary to achieve satisfactory recordings.

Introduction

The recording of extracellular electrophysiological potentials with photoetched electrodes integrated into the floor of the tissue culture chamber is an attractive technique that should allow the long-term monitoring of neuronal activity in explant as well as dispersed cell culture. The main advantages of this new technique are the potential for simultaneous recording from and stimulation of a large number of neurons, the elimination of vibrations between recording electrode and signal source, the ability to carry out experiments in closed, sterile chambers, and the ability to carry out high-power microscopy during recording.

Chambers containing photoetched electrodes have been used to record field potentials from cultured cardiac muscles (Thomas et al., 1972), to monitor simultaneous single unit activity from snail ganglia (Gross, 1979; Gross et al., 1977), and to record evoked action potentials from dissociated mammalian ganglionic neurons (Pine, 1980). However, no laboratory has so far achieved recordings from mammalian CNS neurons cultured on the electrode surface. This important step in

0165-0270/82/0000–0000/$02.75

demonstrating the usefulness of this new electrophysiological technique has been hindered by a variety of neurobiological and technical difficulties such as insulation breakdown after days under warm saline, electrode reinsulation by vigorous glia growth, poor cellular adhesion to the most stable insulation materials and the monitoring of signals from the relatively small CNS neurons. It is the purpose of this paper to report recently developed procedures that have allowed the monitoring of mouse spinal neurons for several days with photoetched electrodes.

Materials and methods

Insulation of multimicroelectrode surface

From our experience, hydrophilic insulation materials swell in saline and usually reveal an unacceptable drop in shunt impedance within minutes to hours after exposure to the culture medium. The insulation material we have found most stable under saline at 37°C is a highly hydrophobic polysiloxane resin (Dow Corning DC 648). Deinsulation of the tips of the gold electrodes in the area of the recording matrix was performed using single shots from an ultraviolet laser (337.1 nm) at an energy density of $4\,\mu J/\mu m^2$ (Gross, 1979). Usually 2–4 electrodes were left insulated so that shunt impedances might be checked periodically as an indicator of insulation stability (Gross, 1979). Electrode impedances (Z) ranged from 4 to 12 MΩ with an average Z of 6 MΩ. Recording electrode impedances have so far not exceeded 7 MΩ.

Preparation of insulated surface for culturing

Due to its hydrophobic nature the polysiloxane resin does not permit good cell adhesion. However, a 1 s exposure of the recording area to temperatures above 1500°C produces a hydrophilic oxidation layer to which cells adhere more readily.

Tissue culture

Spinal cord tissue was isolated and dissociated from 13- to 15-day mouse embryos (GIBCO HA/ICR) according to the procedure of Ransom et al. (1977) with the following modifications. Seven to twelve spinal cords were pooled in 1 ml Hanks BBS containing 2% penicillin–streptomycin during dissection. The tissue was transferred to a dry, sterile petri dish and minced with scalpels. It was then transferred to 1.5 ml of Eagle's Minimum Essential Medium (GIBCO, Earle's liquid), fortified with 10% heat-inactivated horse serum (GIBCO) and 10% fetal calf serum (GIBCO), and buffered for 5% CO_2 atmosphere. The tissue was further dissociated by trituration with Pasteur pipettes (10–12 times). Of the 3 ml final suspension volume 1 ml was plated directly on the multimicroelectrode plate (MEP) and was confined by a 1 mm thick silicone gasket forming a plating area of 600 mm^2. Fluorodeoxyuridine (FdU) plus uridine was added 48 h after plating in the concentrations recommended by Ransom et al. (1977). The first medium changes were carried out within 3–6 days after seeding with MEM containing 10% horse serum. In all medium changes only 50% of the old medium was removed and replaced.

Fig.
cham
to th
medi
screw

rophysiological technique has been
hnical difficulties such as insulation
trode reinsulation by vigorous glia
table insulation materials and the
NS neurons. It is the purpose of this
that have allowed the monitoring of
toetched electrodes.

materials swell in saline and usually
ance within minutes to hours after
material we have found most stable
olysiloxane resin (Dow Corning DC
ctrodes in the area of the recording
an ultraviolet laser (337.1 nm) at an
lly 2–4 electrodes were left insulated
iodically as an indicator of insulation
Z) ranged from 4 to 12 MΩ with an
ances have so far not exceeded 7 MΩ.

xane resin does not permit good cell
cording area to temperatures above
r to which cells adhere more readily.

ed from 13- to 15-day mouse embryos
re of Ransom et al. (1977) with the
al cords were pooled in 1 ml Hanks
uring dissection. The tissue was trans-
ith scalpels. It was then transferred to
(GIBCO, Earle's liquid), fortified with
d 10% fetal calf serum (GIBCO), and
was further dissociated by trituration
ml final suspension volume 1 ml was
te (MEP) and was confined by a 1 mm
f 600 mm^2. Fluorodeoxyuridine (FdU)
the concentrations recommended by
ges were carried out within 3–6 days
se serum. In all medium changes only
laced.

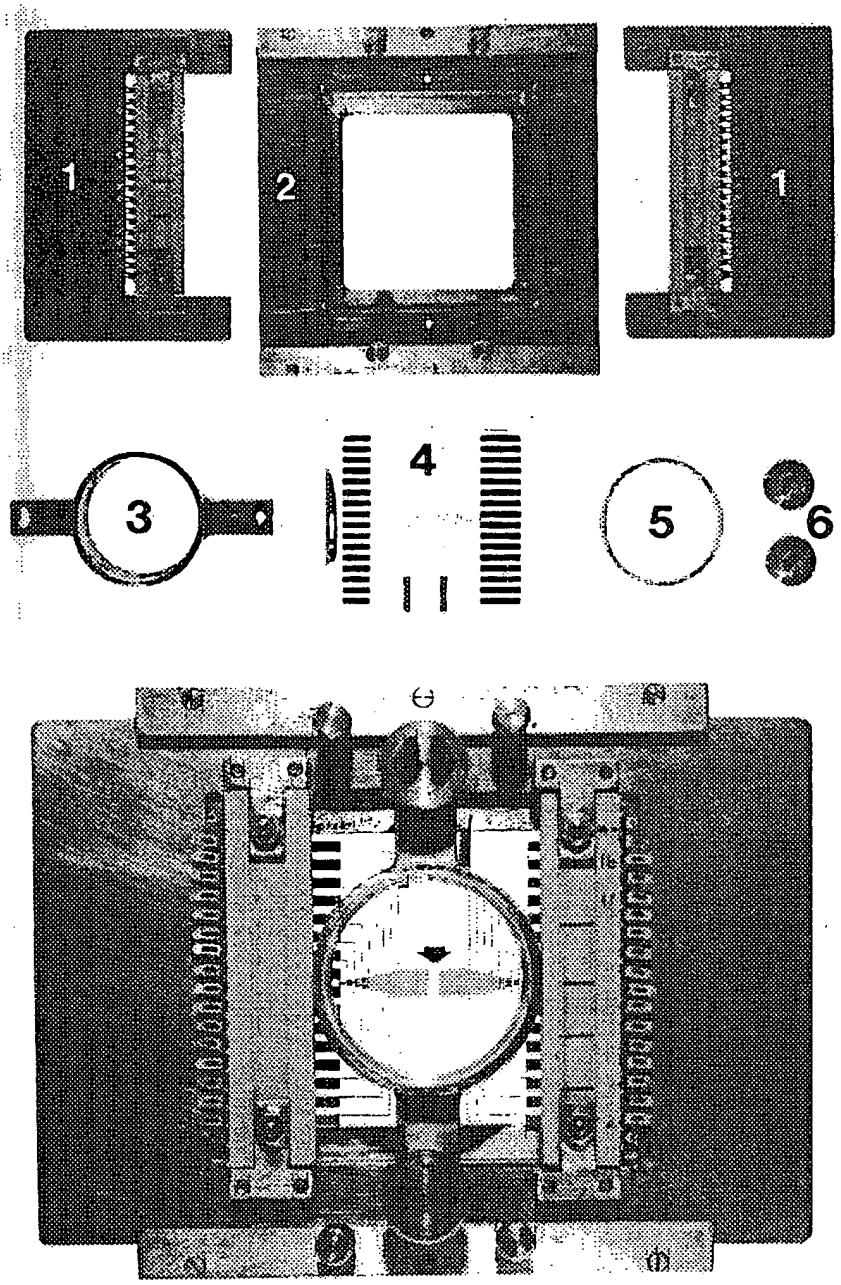

Fig. 1. Disassembled (top) and assembled (bottom) culture and recording chamber. The floor of the chamber is a glass multimicroelectrode plate containing 36 gold photoetched electrodes. The arrow points to the recording matrix shown with cultured cells in Fig. 2. 1, contact strips; 2, electrode plate holder; 3, medium retaining ring; 4, multielectrode plate (50×50×1.5 mm); 5, silicone 'O' ring; 6, attachment screws.

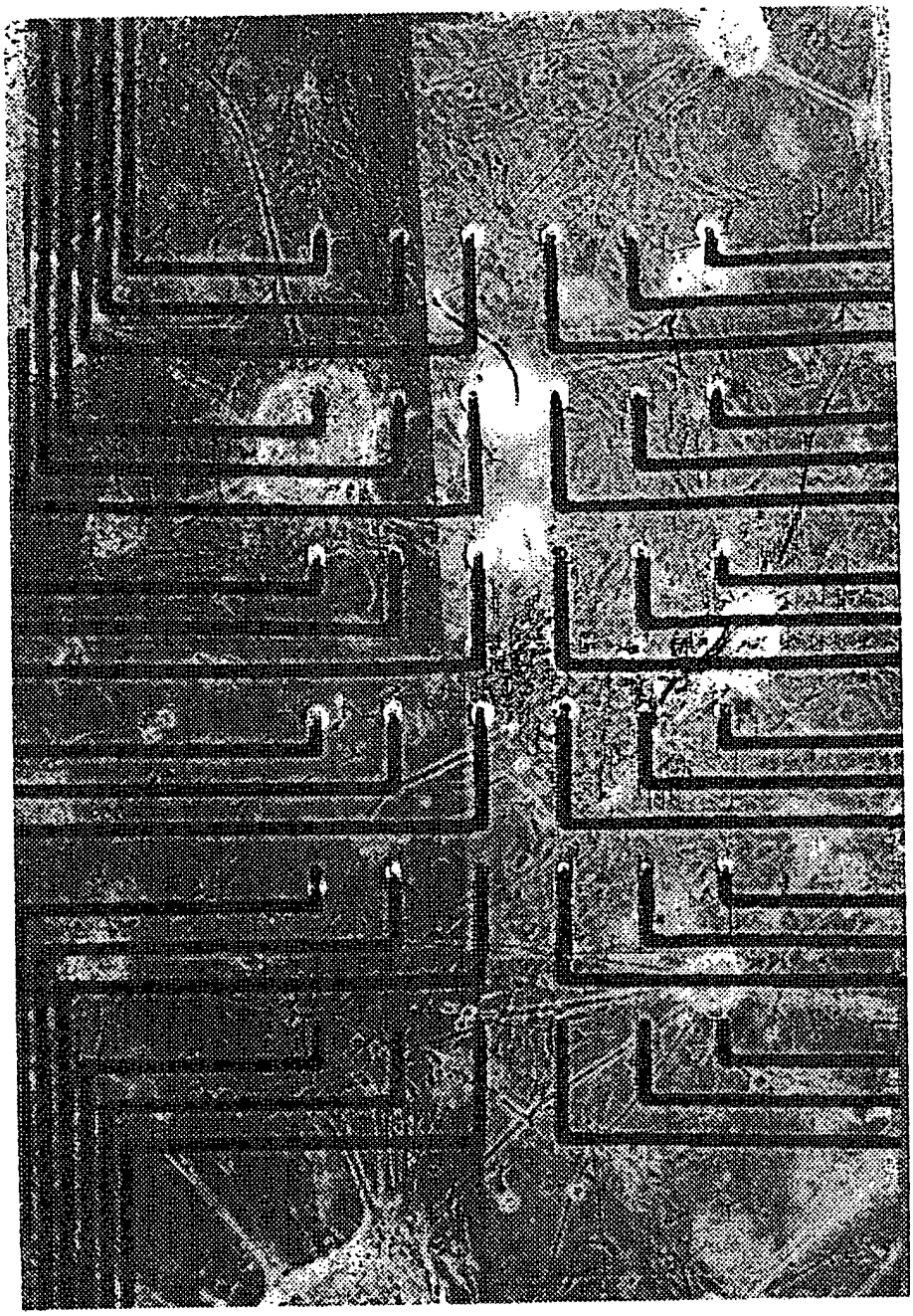

Fig. 2. Inverted microscope view of recording matrix showing the 36 microelectrodes (12 μm wide) and a variety of neuronal aggregates, small tissue fragments as well as a developing glia carpet 10 days after plating dissociated embryonal spinal cord segments on the multielectrode surface. The electrode tips are spaced 90 μm laterally and 180 μm longitudinally. All conductors except those of the bottom row have been deinsulated with single laser shots. The halos of the deinsulation craters are visible at the tips of most conductors. The bright areas between the left and right halves of the recording matrix at the level of rows 2 and 3 are inhomogenicities in the insulation layer and do not represent cell aggregates.

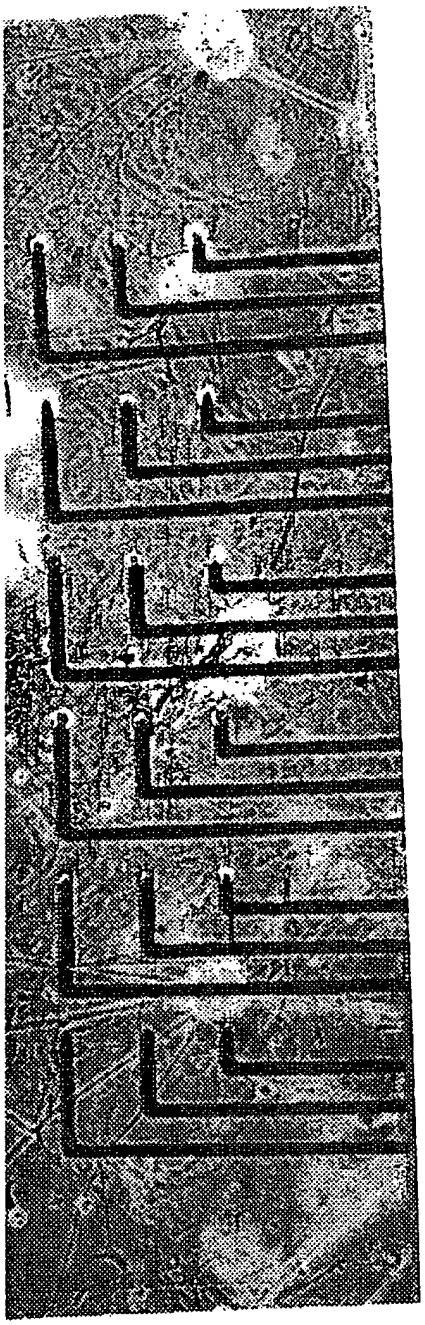

lowing the 36 microelectrodes (12 μm wide) and a as well as a developing glia carpet 10 days after the multielectrode surface. The electrode tips are conductors except those of the bottom row have the deinsulation craters are visible at the tips of right halves of the recording matrix at the level of er and do not represent cell aggregates.

Arrangements for electrophysiological recording

Prior to recording, the silicone gasket was replaced by a stainless-steel ring 28 mm in diameter that served as the chamber wall and ground electrode (see Fig. 1). Standard arrangements for signal amplification and oscilloscope display were used. During recording the culture medium was maintained at the proper pH and oxygen tension by a 20 ml/min moist flow of 5% CO_2, 35% O_2 and 60% N_2. Temperature within the recording chamber was maintained between 35 and 36°C except when deliberately varied with a microscope stage heater (Reichert) connected to a DC power supply.

Results

Fig. 2 shows an inverted microscope view of mouse spinal tissue from 13-day embryos 10 days after seeding. Recordings were obtained from the clump of cells overlying the first electrode from the left in the second row (designated E21) which had an impedance of 7 MΩ.

Although Fig. 2 shows few identifiable neuronal profiles, the large number of fine processes originating from cell clumps or aggregates is indicative of a healthy culture. The tissue fragment centered on E21 is unfortunately too dense to allow identification of neurons. However, the diffraction patterns discernible within the fragment reveal most cell bodies to be below 15 μm diameter. Glial cells are well established in most regions of the recording matrix but have been prevented from overgrowing the culture by FdU added two days after seeding.

Representative extracellular electrophysiological recordings are shown in Fig. 3. All recordings shown were obtained from electrode 21 of Fig. 2 over a 48 h period. It can be seen that the electrode is monitoring complex spontaneous activity from several cells. No such activity was seen by any other electrode of the matrix. It is interesting that E22, situated only 20 μm from the edge of the active tissue fragment, is not monitoring any spike potentials (Fig. 3A). The microfragment exhibited a variety of activities ranging from rhythmic multi-unit bursts (Fig. 3B and C) to long periods of intensive multi-cell firing (Fig. 3D) during which time the bursting usually ceased. The largest spikes recorded were 200 μV in amplitude.

Fig. 4 depicts spontaneous activity recorded from a thin sheet of spinal cell aggregates (12-day culture from 15-day mouse embryos). A photograph of this cell layer in the area of the recording electrode is shown in Fig. 5. In this case the activity was not complex and represented the regular firing of one or two single units. Changes in the frequency of spiking in response to a gradual lowering of the temperature over a period of 1 h as well as to the addition of sodium citrate (in a 25 mM concentration) demonstrated that this activity was biological in nature and not an artifact of the recording system. Fig. 4A and B shows activity at 34°C and 20°C respectively. During the period of cooling, spike frequency decreased from 17 to less than 2 spikes/10 s interval. Return to 34°C (Fig. 4C) resulted in total recovery of activity but with some loss of spike amplitude. These changes in firing frequency are depicted graphically in Fig. 6. Fig. 4D shows the effect of sodium citrate addition

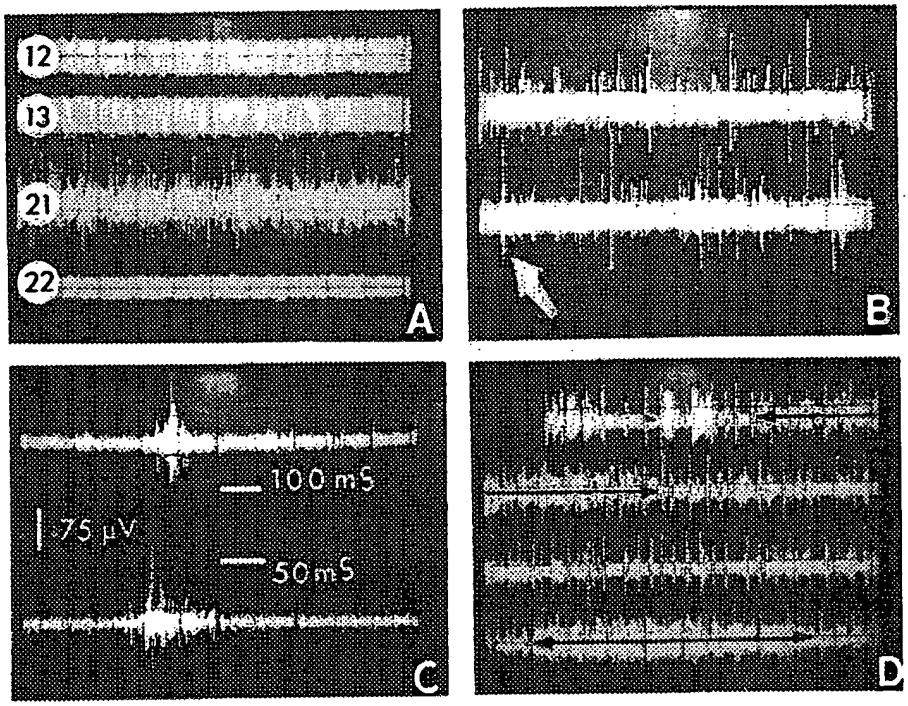

Fig. 3. Spontaneous extracellular activity recorded from 150 μm tissue fragment situated over the electrode in row 2 and column 1 (denoted E21) of the recording matrix shown in Fig. 2. Oscilloscope traces are sequential and do not represent simultaneous recordings. A: comparison of activity on adjacent electrodes in rows 1 and 2 on the left half of the recording matrix. Calibration: 1 s/div, 40 μV/div. B: typical activity with maximum signal amplitudes of 190 μV and noise levels of 30 μV. Calibration: 2 s/div, 40 μV/div. C: multi-unit bursts that appear as single spikes in B (at arrow). D: slow sweep (5 s/div) showing changes from bursting to long periods of intensive multi-unit activity (horizontal arrows).

which resulted in an increase of bursting, a decay of spike amplitude and finally the irreversible termination of activity.

Discussion

These recordings represent the first monitoring of activity with photoetched electrodes from mammalian spinal tissue in culture. Furthermore, the observations were limited to 2 days for technical reasons or by the deliberate termination of cultures to verify the bioelectric origin of the signals. Minor modification in procedures could easily expand the recording period. Recordings have also been obtained from dissociated mouse brain tissue; however, on these occasions the signal-to-noise ratios did not exceed 1.8 : 1. The increase in signal-to-noise ratios seen

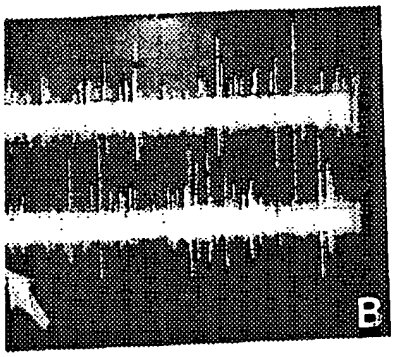

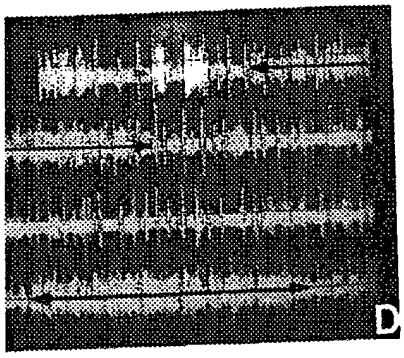

n 150 μm tissue fragment situated over the recording matrix shown in Fig. 2. Oscilloscope ecordings. A: comparison of activity on adjacent ing matrix. Calibration: 1 s/div, 40 μV/div. B: 0 μV and noise levels of 30 μV. Calibration: s single spikes in B (at arrow). D: slow sweep ods of intensive multi-unit activity (horizontal

ecay of spike amplitude and finally the

nitoring of activity with photoetched culture. Furthermore, the observations ns or by the deliberate termination of f the signals. Minor modification in ing period. Recordings have also been ssue; however, on these occasions the he increase in signal-to-noise ratios seen

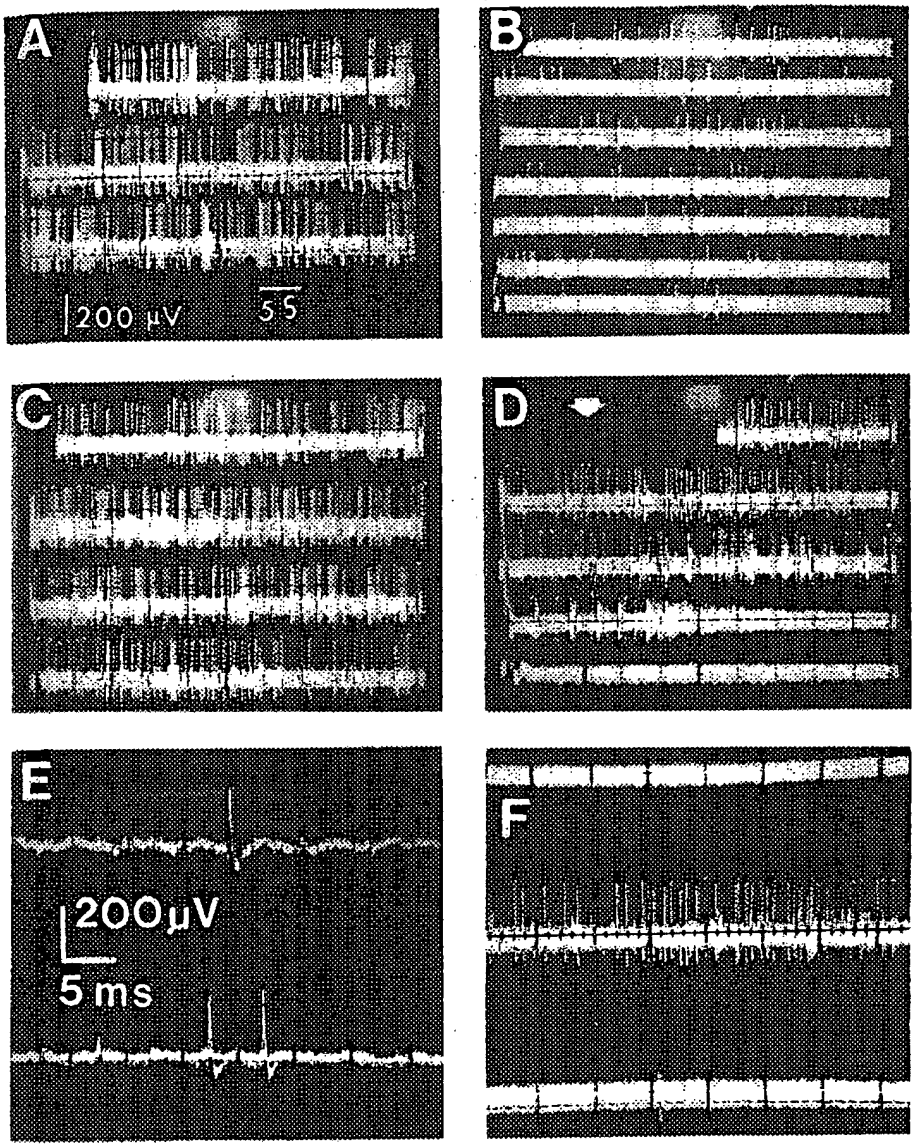

Fig. 4. Spontaneous extracellular activity from a thin sheet of aggregated spinal cells 12 days after dissociation and seeding. Recordings were obtained with the photoetched electrode identified in Fig. 5 (impedance: 4 MΩ). Calibration: A–D sweep 5 s/div; amplitude: 195 μV/div; band width: 100–10,000 Hz. Display resulting from sequential traces on storage oscilloscope. A: single-unit activity at 34°C. B: activity on same electrode 1 h later with temperature lowered to 20°C. C: recovery of activity with temperature restoration to 34°C over a 30 min period. D: reaction of active unit to addition of citrate (at arrow). Note rhythmic bursting after a 110 s interval followed by a decrease in spike amplitude and complete cessation of activity. E: rapid sweeps depicting single action potentials (band width: DC 10,000 Hz plus 60 Hz filter) with maximum amplitudes of 360 μV and a signal-to-noise ratio of 8:1. F: signals from 3 adjacent electrodes located under the thin tissue sheet shown in Fig. 5. Only the center electrode is monitoring activity (arrow in fig. 5).

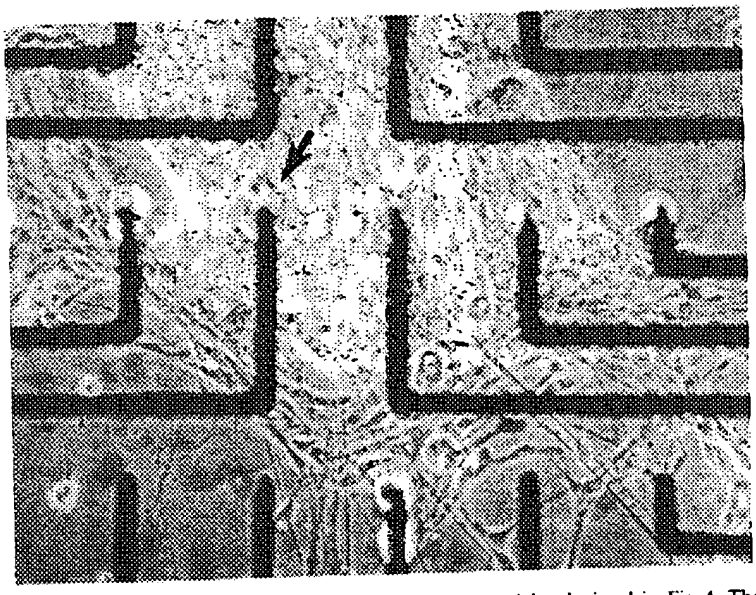

Fig. 5. Inverted microscope view of region producing activity depicted in Fig. 4. The tissue is almost a monolayer formed by reaggregated mouse spinal cord cells. The active unit, however, could not be identified. The arrow points to electrode with which data in Fig. 4 was obtained. Electrodes to either side did not monitor activity.

recently may be due to the introduction of the surface oxidation of the insulation layer which has resulted in improved cell-to-substrate adhesion. The usefulness of this as a general technique for promoting cell adhesion as compared to other methods of surface modification (collagen, polylysine, etc.) is currently under investigation in this laboratory and will be reported in a separate paper.

Although the characteristics of the activity shown in Figs. 3 and 4 would clearly

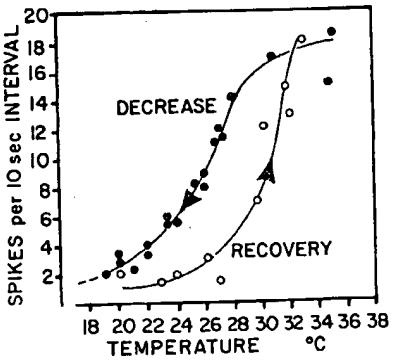

Fig. 6. Temperature dependence of spontaneous activity recorded from neuron described in Figs. 4 and 5. Temperature was lowered at 0.3°C/min and raised at 0.5°C/min.

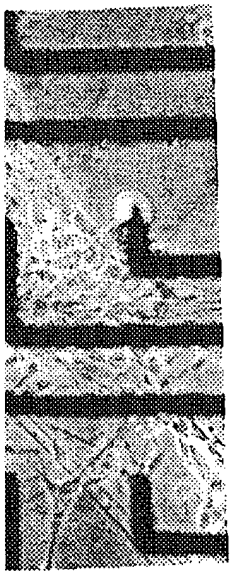

vity depicted in Fig. 4. The tissue is almost a
cells. The active unit, however, could not be
n Fig. 4 was obtained. Electrodes to either side

ie surface oxidation of the insulation
substrate adhesion. The usefulness of
cell adhesion as compared to other
polylysine, etc.) is currently under
orted in a separate paper.
shown in Figs. 3 and 4 would clearly

recorded from neuron described in Figs. 4 and 5.
5°C/min.

be accepted as neuronal if recorded with standard metal electrodes, the introduction of a new recording technique demands greater caution. We have, therefore, attempted to demonstrate the biological origin of the signals with simple physical and chemical manipulations as already described in the Results section. The temporary increase in activity together with a decrease in spike amplitude and finally cessation of firing is a typical reaction to high concentrations of sodium citrate, a known calcium ion chelator. The temperature dependence of the spontaneous firing frequency and the spike amplitude is also typical of neurons (Gähwiler et al., 1972; Leiman and Seil, 1973). Most cells stop firing below 20°C, although not all cells display a temperature-dependent spontaneous firing pattern between 25 and 38°C. As far as recording system noise is concerned, none of the major categories (white noise, current or 1/f noise, and shot noise) are known to display sigmoidal dependence on temperature (Neher, 1974; DeFelice, 1981).

We have achieved satisfactory signal-to-noise ratios without the use of platinum black which, up to now, has been generally utilized as a means lowering electrode impedances (Thomas et al., 1972; Pine, 1980). In view of the inherent instability of such electrode tips (Gesteland et al., 1959; Robinson, 1968), the use of platinum black should be avoided if the long-term monitoring of signals is a major objective.

The multielectrode plates used in these experiments are obviously designed for the long-term, simultaneous recording of spike activity from cultured neuronal monolayers in which the active units and most of their interconnections can be identified and observed. Furthermore, we are developing laser microbeam cell surgery techniques that will allow the simplification of the monolayer or a change in neuronal interconnections during recording (Higgins et al., 1980). In this paper we have taken the initial electrophysiological step by demonstrating that mammalian CNS tissue can be satisfactorily coupled to a polysiloxane insulation layer and that good signal-to-noise ratios can be obtained. Although preliminary data indicate that healthy-appearing cultures can be maintained on the polysiloxane for over 3 weeks, we cannot yet make any statements about signal acquisition during that period of time. Monolayers and presumably the surfaces of tissue microfragments are not morphologically stable. Glial movement and elastic readjustments will probably cause a shifting of active units relative to the recording crater. The reinsulation of these electrode craters is also a problem that may be decreasing the probability of simultaneous recording and to which the FdU treatment appears to be only a partial solution. Nevertheless, the advantages of recording with multimicroelectrode surfaces in culture are substantial and justify a serious attack on these problems. There is no other approach that will give us the capability of long-term, continuous monitoring, stimulation and observation of over 30 neurons in a controlled chemical environment. Neither the conventional methods of recording nor the utilization of voltage-sensitive dyes offer such a combination of advantages.

Acknowledgements

The authors wish to thank Mr. Andy Pratt for his technical assistance. We also thank the Siemens Corporation of Munich, Germany for the gratuitous production

of the photoetched plates in 1976. Some plates can still be utilized after 4 years of experimentation. We acknowledge the assistance of the Sandoz Corporation of Basel, Switzerland and specifically thank Dr. Meier-Ruge for making available a UV laser microbeam system.

Finally, we are grateful for the critical support from NINCDS through NIH Grant [redacted]

References

DeFelice, L.J. (1981) Introduction to Membrane Noise. Plenum Press, N.Y., chapter 5.

Gähwiler, B.H., Mamoon, A.M., Schlapfer, W.T., and Tobias, C.A. (1972) Effects of temperature on spontaneous bioelectric activity of cultured nerve cells, Brain Res., 40:527–533.

Gesteland, R.C., Howland, B., Lettvin, J.Y. and Pitts, W.M. (1959) Comments on microelectrodes, Proc. IRE, 47:1856–1862.

Gross, G.W. (1979) Simultaneous single unit recording in vitro with photoetched, laser deinsultaed gold multi-microelectrode surface, IEEE Transact. Biomed. Engng, BME 26:273–279.

Gross, G.W., Rieske, E., Kreutzberg, G.W., and Meyer, A. (1977) A new fixed array multimicroelectrode system designed for long term monitoring of extracellular single unit neuronal activity in vitro, Neurosci. Lett., 6:101–105.

Higgins, M.L., Smith, M.N. and Gross, G.W. (1980) Selective cell destruction and precise neurite transection in neuroblastoma cultures with pulsed UV laser microbeam irradiation: an analysis of mechanisms and transection reliability with light and scaning electron microscopy, J. Neurosci. Meth., 3:83–99.

Leiman, A.L. and Seil, F.J. (1973) Spontaneous and evoked bioelectric activity in organized cerebellar tissue culture, Exp. Neurol., 40:748–758.

Neher, E. (1974) Elektronische Messtechnik in der Physiologie, Springer, Berlin, pp. 53–55.

Pine, J. (1980) Recording action potentials from cultured neurons with extracellular microcircuit electrodes, J. neurosci. Meth., 2:19–31.

Ransom, B. R., Neale, E., Henkart, M., Bullock, P.N. and Nelson, P.G. (1977) Mouse spinal cord in cell culture I. Morphological and intrinsic neuronal electrophysiological properties, J. Neurophys., 40:1132–1150.

Robinson, D.A. (1968) The electrical properties of metal microelectrodes, Proc. IEEE, 56:1065–1071.

Thomas, C.A., Jr., Springer, P.A., Loeb, G.E. , Berwald-Netter, Y. and Okun, C.M. (1972) A miniature microelectrode array to monitor the bioelectric activity of cultured cells, Exp. Cell Res., 74:61–66.

STIC-ILL

From: Baskar, Padmavathi
Sent: Thursday, May 02, 2002 8:10 AM
To: STIC-ILL
Subject: 08913811

COULD YOU PLEASE GET THESE REFERENCES AS AN URGENT ORDER. THANKS FOR ALL THE HELP.

Gross et al. (J. of Neuroscience Methods 5: 13-22, 1982)

Ambros-Ingerson et al (Brain Research (1993) 620:237-244).

Padma Baskar
Art Unit 1645
Patent Examiner/Biotechnology
CM-1, 8E-13, BOX 8E-12
703-308-8886

Article title	Waveform analysis suggests that LTP alters the kinetics of synaptic receptor channels
Article identifier	0006899393011709
Authors	Ambros_Ingerson_J Xiao_P Larson_J Lynch_G
Journal title	Brain Research
ISSN	0006-8993
Publisher	Elsevier Netherlands
Year of publication	1993
Volume	620
Issue	2
Supplement	0
Page range	237-244
Number of pages	8
User name	Adonis
Cost centre	Development
PCC	$20.00
Date and time	Thursday, May 02, 2002 12:48:43 PM

Brain Research, 620 (1993) 237–244

BRES 19136

Waveform analysis suggests that LTP alters the kinetics of synaptic receptor channels

José Ambros-Ingerson, Peng Xiao, John Larson and Gary Lynch

Center for the Neurobiology of Learning and Memory, University of California, Irvine, CA 92717 (USA)

(Accepted 23 March 1993)

Key words: Long-term potentiation; Hippocampus; Glutamate receptor; Channel kinetics; Decay time constant; Paired-pulse facilitation; Release kinetics

The waveform of an isolated excitatory monosynaptic response reflects the kinetics of transmitter release, the kinetics of synaptic receptor channels and the filtering properties of neurons. Results reported here indicate that long-term potentiation (LTP) causes correlated decreases in the rise time and decay time constant of synaptic potentials recorded in hippocampal slices in which inhibitory currents and post-synaptic spiking were suppressed. Statistical comparisons of waveforms revealed that the distortions introduced by LTP could be corrected by stretching the time-scale of potentiated responses according to the percent change in the decay time constant. The LTP associated decrease in the decay time constant also obtained in slices from immature hippocampus which contain spines and dendrites greatly simplified from those of the adult. Hence, filtering properties of spines are not likely involved in the effect. Paired-pulse facilitation (PPF), a transient increase in transmitter release, did not reproduce the waveform effects of LTP but did cause a slight leftward shift of the response. These results suggest that LTP modifies the kinetics of receptor channels, and that PPF accelerates release.

INTRODUCTION

Long-term potentiation (LTP), a phenomenon widely studied as a possible substrate for memory, involves a remarkably stable increase in the slope and amplitude of synaptic potentials[4]. Recent studies of the hippocampus indicate that LTP also reduces the decay time constant (decay τ) of the AMPA (glutamate) receptor-mediated component of the synaptic response[1]. Increasing the size of the responses by stimulating more synapses or enhancing release did not affect the decay τ[1]. These results are potentially diagnostic with regard to the substrates of LTP because the decay τ of synaptic currents is directly related to the mean open time of transmitter receptor channels[2,9], a point that has been confirmed for hippocampal synapses[1,16]. Thus, the observed change in the decay τ constitutes evidence that LTP modifies AMPA receptors. Since channel closing is probabilistic, shorter mean open times should alter all phases of the synaptic waveform and do so in a predictable fashion. The extensive literature on LTP contains no suggestions for effects of these kinds which led us to test for them in the experiments described here. In addition, we also tested if the decay τ change occurs in association with LTP across very different biophysical environments, as expected if it is due to receptor modifications. Paired-pulse facilitation (PPF), a transient form of response enhancement due to increased transmitter release[7,18] was used as a control, and this resulted in a novel observation regarding this well-studied phenomenon.

MATERIALS AND METHODS

Hippocampal slices were prepared from male Sprague–Dawley rats and maintained at 35±1°C in medium containing in mM: NaCl 124, KCl 3, KH_2PO_4 1.25, $NaHCO_3$ 26, $CaCl_2$ 3.4, $MgSO_4$ 2.5, D-glucose 10, and L-ascorbic acid 2. Field CA3 was surgically separated, and stimulating electrodes were positioned to activate separate populations of Schaffer/commissural fibers with synapses in the apical dendritic region of field CA1b. The slices were infused with picrotoxin (50 μM) and 2-hydroxy-saclofen (100 μM) to block IPSPs mediated by $GABA_A$ and $GABA_B$ receptors, respectively. Whole-cell patch clamp studies have shown that hyperp larizing currents are blocked by these agents under the experimental conditions used in the present experiments (unpublished data). Tetrodotoxin (10 μM) was ejected by pressure from a micropipette positioned in the

Correspondence: J. Ambros-Ingerson, CNLM, University of California, Irvine, CA 92717, USA. Fax: (1) (714) 856-8481.

basal dendritic zones at the same medio-lateral level as the recording electrode to block action potentials. LTP was elicited by theta burst stimulation[8] delivered to one of the two pathways after a baseline recording period (one stimulation pulse every 20 s) sufficiently long (usually 20–30 min) to establish that synaptic responses were stable. Two stimulation pulses separated by 75 ms (on the same pathway) were used to elicit paired pulse facilitation. In the hetero-synaptic paired pulse experiments, the same experimental configuration was utilized, except that the first pulse was delivered to an alternate pathway, and the response to the second pulse was compared to the response to the first pulse for the pathway under consideration.

Field EPSPs were filtered at 10 kHz, digitized at 10 kHz and stored on computer media. Waveform measurements were carried out in a Sun4/110 workstation from averages of from 8 to 16 successive field EPSPs collected shortly before (for both control and paired-pulse facilitation) and 10–40 ($\bar{x} = 22$) min after inducing LTP.

The estimate of the decay τ constant was obtained by least-squares fit of $v(t) = Ae^{-t/\tau}$ to the data set $\{(t_i, v_i)$: $t_i > t_p$ and $0.9 \geq v_i / v_p \geq 0.3\}$ where v_i is the recorded voltage at time t_i, and t_p and v_p are the time and voltage at peak amplitude, respectively, by means of the Levenberg–Marquardt non-linear method[10,13]. This corresponds to fitting a single exponential to the decaying portion (90% to 30%) of the recorded field potential. The 90% to 50% decay τ was also evaluated for each experiment. Experiments where these two estimates differed by more than 1 ms were not used in the study. Refined estimates of time and voltage at peak amplitude (t_{pk}, v_{pk}) were obtained as the coordinates of the minimum of the least-squares fit of a second degree polynomial (i.e. $p(t) = a_0 + a_1 t + a_2 t^2$) to the data set $\{(t_i, v_i)$: $0.85 \leq v_i / v_p\}$. The time to 70% of peak amplitude ($t.7$) was estimated as the root $t = p^{-1}(0.7v_{pk})$ that satisfies $t \in [t_{\min i \in F}, t_{\max i \in F}]$ where $p(t)$ is the second degree polynomial least-squares fit to the data set $\{(t_i, v_i)$: $i \in F\}$ and $F = \{i: t_i < t_p$ and $0.6 \leq v_i / v_p \leq 0.8\}$. The estimate of $t.9$ was obtained similarly as $t = p^{-1}(0.9v_{pk})$ for the set $F = \{i: t_i < t_p$ and $0.8 \leq v_i / v_p < 1.0\}$.

The normalized subtraction trace $s(t)$ of the control $c(t)$ and experimental $e(t)$ responses was obtained as $s(t) = (n_e(t) - n_c(t))(\text{largest}(n_e(t) - n_c(t))^{-1}$ where $n_c(t) = -1$ mV$(c_{pk})^{-1} c(t + t_{pk})$ is the normalized control trace with peak amplitude of -1 mV at time $t = 0$, and $n_e(t) = -1$ mV$(e_{pk})^{-1} e(t + t_{pk})$ is the experimental response scaled to the same amplitude and the same zero time reference as $n_c(t)$ (assuming $e(t)$ and $c(t)$ are not zero within the time interval under consideration). The mean normalized subtraction trace was obtained as $\bar{s}(t) = n^{-1} \Sigma_{i=1}^{n} s_i(t)$ where $s_i(t)$ is the normalized subtraction trace for experiment i. The standard deviation trace was obtained analogously.

The time translation of response $v(t)$ is given by $v_r(t + t_r) = v(t)$ and its dilation by $v_s(t(1 + t_s)) = v(t)$, where t_r is the translation time value and t_s is the dilation factor. Cubic spline interpolation was used to estimate the voltage of the original response at arbitrary time values. The time transformations were performed on the experimental trace using $t_r = t.9_{control} - t.9_{exp}$ for time translation (shift) and $t_s = ((\tau_{control} / \tau_{exp}) - 1)$ for time dilation (stretch).

The deviation error D_e can be defined as $D_e = (t_2 - t_1)^{-1} \int_{t_1}^{t_2} |s(t)| dt$, where $s(t)$ is the normalized subtraction trace and $[t_1, t_2]$ is the time interval under consideration. Note that, as defined, D_e satisfies the properties of a metric (e.g. non-negativity, symmetry, triangle inequality) for the space of traces scaled to the same amplitude[14]. The deviation errors D_e in Fig. 2 were estimated by numerical integration using the interval $[-3,12]$ ms.

RESULTS

In vitro slice experiments were conducted using extracellular stimulation and recording of the Schaffer-commissural synapses in the surgically isolated hippocampal field CA1, in the presence of picrotoxin (50 μM) and 2-hydroxy-saclofen (100 μM) to block fast and slow inhibitory currents, and local applications of tetrodotoxin in the basal dendritic zones to prevent action potentials in the target cells[1]. Low levels of stimulation current were used to further minimize the likelihood of activating post-synaptic spiking. Intracellular recordings confirm that EPSPs occur in the absence of hyperpolarizing responses or spikes under these conditions. Fig. 1A shows typical averaged field EPSPs before and 20 min after induction of LTP; the superimposed open circles correspond to the single exponential fit using the measured 90–30% decay time constant (τ) and, as shown, there is good agreement between the estimated and actual decay rate. There is a detectable decrease in the decay τ after LTP (-0.47 ms). Having obtained the result described in the earlier report[1], we asked if LTP changes the early as well as the late phase of the response, as expected for a receptor effect. Fig. 1Ai shows the before and after LTP responses scaled to the same amplitude where discrepancies between the two waveforms, both before and after peak amplitude, are evident. The 70% ($t.7$) and 90% ($t.9$) rise times were used to quantify the early time-course of the response; both indices were reduced after induction of LTP. Thus, for this case, LTP affected the entire waveform of the synaptic response and not simply the late component used to measure the decay τ. Fig. 1Ai shows a third trace which is a 'time stretch' of the potentiated response using the percent change in the decay τ as the stretching parameter. Note that this causes the potentiated waveform to align almost exactly with the pre-LTP record. The significance of this observation is discussed below.

We next tested if the LTP-induced changes in the early and late phases of the synaptic waveform are correlated. Results for 17 experiments are shown in Fig. 1Aii with the decay τ change on the x axis and the change in the $t.9$ rise-time on the y axis (LTP minus control for each index). A significant correlation ($r_s = 0.64$; $P < 0.01$ t-test based on Spearman's rank order correlation r_s) is present; thus the effects of LTP on different phases of the synaptic waveform are statistically related. The relevance of the correlation between these variables is reinforced by the near zero y-intercept of the linear least-squares fit ($m = 0.35$, $b = -0.07$ ms, $y = mx + b$; dashed line in Fig. 1Aii) indicating that one variable changes only when the other does. On the other hand, the value of the slope of the linear regression indicates that an (absolute) change in decay τ is accompanied by a somewhat smaller change in the rise-time after LTP-induction. The significance of this relation is explored further below when the time stretching transformation is introduced and later in the discussion. In 14 of the 17 LTP cases (not shown), a

convergent control input was available for which we did not observe changes in amplitude ($-3.2 \pm 7.6\%$), decay τ (-0.05 ± 0.28 ms), $t.7$ (0.00 ± 0.07 ms) or $t.9$ (0.03 ± 0.10 ms; $\bar{x} \pm$ S.D.), when LTP was induced on the experimental pathway.

Fig. 1B shows the effects of paired-pulse facilitation (75 ms delay between pulses) on the same control response illustrated in Fig. 1A. The decay τ of the second (facilitated) response was nearly identical to that of the first (control) response, confirming that the effect of LTP on this measure is not due to a simple increase in synaptic currents. Fig. 1Bi shows the first and second responses normalized for peak amplitude. Note that while the waveforms are nearly superimposable, that for the facilitated potential is shifted very slightly to the left. This was detected as a small reduction in both $t.7$ and $t.9$. Fig. 1Bii summarizes the results for changes in the decay τ and $t.9$ for 20 paired pulse facilitation experiments, 14 of which used the pathways employed for the LTP experiments; as indicated, the reduction of $t.9$ for the facilitated response (y axis) was reliably obtained and did not correspond to changes in the decay τ ($P > 0.1$). In an additional 12 cases, where paired-pulse stimulation was delivered hetero-synaptically (i.e. the first pulse was delivered to an alternate pathway), no change was observed in the amplitude ($0.3 \pm 1.2\%$), decay τ (0.09 ± 0.15 ms), $t.7$ (0.00 ± 0.02 ms) or $t.9$ (0.00 ± 0.04; $\bar{x} \pm$ S.D.) measures of the second response (not shown).

Table I provides a statistical summary of the results. LTP not only reduced the decay τ, but also $t.7$ and $t.9$ ($P < 0.001$ two-tailed paired t-test for each index); it is important to note that the effect of potentiation, in pair-wise comparisons, was significantly larger on $t.9$ than on $t.7$ ($P < 0.001$ two-tailed paired t-test). PPF had no detectable effect on the decay τ but did reduce both $t.7$ and $t.9$ ($P < 0.001$ two-tailed paired t-test) though not differentially. The table also shows that not only is the decay τ measure reduced after induction of LTP when compared to its pre-LTP value, but also when compared to the value obtained for the pre-LTP facilitated response which has a peak amplitude much more similar to that of the potentiated response.

In order to further characterize the observed waveform changes, we note that when two traces have the same time-course and are scaled to the same amplitude, their subtraction results in a zero amplitude trace. Conversely, when their time-courses differ, the subtracted trace deviates from zero. A more exacting measure is to consider their normalized subtraction, where for the voltage at each time point, their difference is normalized as a percent of the larger of the two voltages. The trace of the normalized subtraction can

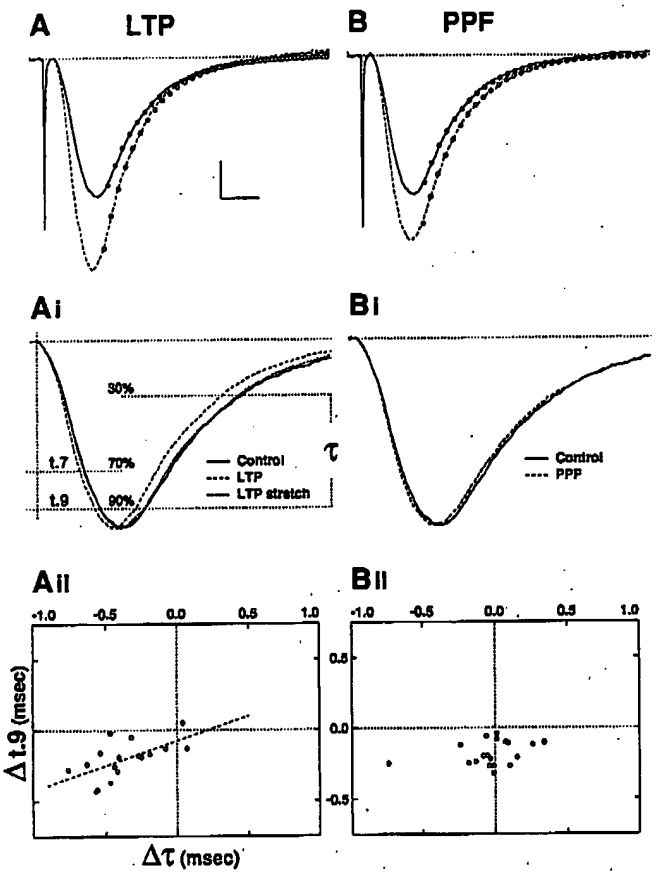

Fig. 1. Effects of LTP and paired pulse facilitation (PPF) on the waveform of synaptic field potentials. A: averaged field EPSPs recorded immediately prior to (solid), and 23 min after, induction of long-term potentiation (LTP, dashed), with their single exponential decay curves (open circles) based on the decay τ measurements. Ai: control (solid) and LTP (dashed) responses in panel A scaled to the same amplitude. The panel illustrates the $t.7$ and $t.9$ measurements as the times, from the initiation of the response, to reach 70% and 90% of peak amplitude, respectively, and the portion of the response that was used to calculate the decay τ. The waveform change after LTP is apparent throughout the response; $t.7$ and $t.9$ were reduced ($\Delta t.7 = -0.33$ ms, $\Delta t.9 = -0.37$ ms) and the decay τ was decreased from $\tau_{control} = 5.83$ ms to $\tau_{LTP} = 5.36$ ms ($\Delta\tau = -0.47$ ms). Time dilation of the LTP trace (dotted), using the percent change in the decay τ as the stretch factor, illustrates the effectiveness of this operation in transforming the LTP time-course into that of the control response. Aii: scatter diagram of the changes in the decay τ versus $t.9$ for the 17 LTP experiments used in the study. The solid circle corresponds to the values obtained for the experiment depicted in panel A. A significant positive correlation was observed between the changes in these indexes when evaluated by Spearman's rank order correlation ($r_s = 0.64$, $P < 0.01$ t-test) and by linear correlation ($r = 0.61$, $P < 0.01$ t-test). The dashed line corresponds to the linear least-squares fit to the data $m = 0.35$, $b = -0.07$ ms, $y = mx + b$). Note the near-zero y-intercept b. B: averaged responses obtained to the first (solid) and second (dashed) stimulation pulses separated by 75 ms (paired-pulse facilitation; PPF) carried out on the same pathway as for the LTP case; the first response is the pre-LTP potential in panel A. Bi: control (solid) and PPF (dashed) responses in panel B scaled to the same amplitude. Note that both $t.7$ and $t.9$ are decreased by PPF ($\Delta t.7 = -0.17$ ms, $\Delta t.9 = -0.22$ ms) whereas the decay τ is virtually unaffected ($\Delta\tau = -0.03$ ms). Bii: as in panel Ai for the 20 PPF experiments used in the study. The solid circle corresponds to the values obtained for the experiment depicted in panel B. No significant correlation was observed between changes in these indexes. Bars = 5 ms, 0.2 mV (A,B); 2.5 ms, arbitrary units (Ai, Bi).

then be used to characterize the waveform changes as a percent difference at each time point, where a positive (negative) deflection indicates that the first (second) response is larger and the percent by which the second (first) response is smaller, and no deflection indicates their agreement.

Fig. 2 illustrates the results of applying the above procedure to the data summarized in Table I. The control and experimental responses were scaled to an arbitrary magnitude of −1 mV and the time at peak amplitude of the control response taken as the zero time reference. Fig. 2A shows the average trace (+S.D. dashed) for 31 control responses normalized as described above.

Fig. 2D shows the mean of the normalized subtraction (+S.D. dashed) results obtained for 31 pairs of control responses taken an average of 14 min apart during baseline recording periods. Note that no deflection away from zero is apparent for the mean trace. The results of applying the same procedure to pre- vs. post-LTP responses for 17 experiments (mean + S.D.) are presented in Fig. 2Ai (upper panel). The changes in $t.7$ and $t.9$ can be seen reflected as a positive deflection before the peak of the response, whereas the decrease in the decay τ appears as a large negative deflection which remains apparent as late as 12 ms after the peak (where the control response has decayed to ~20% of peak amplitude; see Fig. 2A). From this it is apparent that LTP alters the entire waveform of the response.

Fig. 2Ai (bottom panel) shows the averaged (+S.D.) normalized subtractions between the first and second responses in the paired-pulse paradigm for 20 experiments. The positive deflection before the peak corresponds to the reduced values for $t.7$ and $t.9$; the negative deflection after the peak is small, does not grow with time, and disappears late in the response.

Of major interest in understanding the factors that underlie the waveform changes, is the question of whether it is possible to systematically transform the time-course of the experimental response so that it agrees with that of the control response. Two transformations were found useful in accomplishing this: (i) a horizontal stretch or dilation of the response by a constant factor t_s, which corresponds to re-scaling of the time axis, as the voltage at time t is now regarded to be at time $t \times (1 + t_s)$; and (ii) a horizontal shift of the response by a constant value t_r, which corresponds to translation in time, as the voltage at time t is now regarded to be at $t + t_r$. Shifting reduces/increases $t.7$ and $t.9$ equally having no effect on the decay τ whereas stretching reduces/increases all of these measures by approximately the *same percentage* value.

These transformations are illustrated in Fig. 2B, C using the control response described in Fig. 1. In Fig. 2B, the waveform has been stretched (dashed line) by

TABLE I

Summary of the effects of paired pulse facilitation (PPF; 75 ms delay between pulses) and long-term potentiation (LTP) on the waveform of field EPSPs

Shown are the results obtained for three groups of experiments: (i) responses obtained shortly before and an average of 22 min after, induction of long-term potentiation ($n = 17$; control and LTP); (ii) first and second responses in the paired-pulse paradigm ($n = 20$; control and PPF); and (iii) the second response shortly before, and first response an average of 18 min after, induction of LTP for experiments in which both manipulations had a common control response ($n = 14$; pre-LTP-PPF and LTP). The first two columns show the peak amplitude and measured decay τ for each of the aforementioned conditions in each group. The five rightmost columns show the changes in amplitude, decay τ, $t.7$, $t.9$ and $t.9 - t.7$ (i.e. the change in $t.9$ versus the change in $t.7$) as obtained from pair-wise comparisons in absolute values (percent points in parenthesis) between each of the two responses for each experiment in the group (LTP minus control, PPF minus control, and LTP minus pre-LTP-PPF). The decay τ, $t.7$ and $t.9$ measures are illustrated in Fig. 1. Values for all entries are $\bar{x} \pm$S.D.

	n	*Amplitude mV*	τ *ms*	*Change in: (pair-wise comparisons)*				
				Amplitude mV (%)	τ *ms (%)*	*t.7 ms (%)*	*t.9 ms (%)*	*t.9 − t.7 ms*
Control	17	0.85 ± 0.22	6.59 ± 1.20					
				0.48 ± 0.14 (57.9 ± 14.0)	−0.37 ± 0.23 ** (−5.9 ± 3.7)	−0.13 ± 0.11 ** (−4.0 ± 3.3)	−0.20 ± 0.13 ** (−5.0 ± 2.9)	−0.08 ± 0.08 **
LTP		1.33 ± 0.32	6.22 ± 1.29					
Control	20	0.83 ± 0.24	6.58 ± 1.29					
				0.33 ± 0.09 (39.8 ± 8.2)	−0.01 ± 0.23 * (−0.1 ± 3.8)	−0.15 ± 0.05 ** (−4.8 ± 1.6)	−0.18 ± 0.08 ** (−4.4 ± 2.1)	−0.03 ± 0.06 *
PPF		1.16 ± 0.32	6.57 ± 1.28					
pre-LTP-PPF	14	1.13 ± 0.26	6.62 ± 1.29					
				0.15 ± 0.10 (14.3 ± 9.3)	−0.37 ± 0.21 ** (−6.0 ± 3.4)	0.02 ± 0.09 * (0.7 ± 2.9)	−0.01 ± 0.12 * (−0.2 ± 2.9)	−0.03 ± 0.08 *
LTP		1.28 ± 0.27	6.25 ± 1.39					

* $P > 0.1$ not significant, ** $P < 0.001$; two-tailed paired t-test.

the average percent decrease in decay τ that occurs with LTP (in effect contracting its time-course as the stretching parameter is negative; see Table I). Note that the transformation converts the response to its potentiated shape (see Fig. 1) and that normalized subtraction of the control trace from its stretched counterpart (inset) yields a result similar to that for the mean of the post- minus pre-LTP experiments (Fig. 2Ai). Fig. 2Bi shows the effects of applying time stretching to each of the LTP ($n = 17$) and PPF ($n = 20$) experiments. The potentiated or facilitated responses were stretched prior to normalized subtraction by the percent to which their decay τ's differed from those of their associated control responses. Time stretching removed most of the differences in the waveforms of the pre- vs. post-LTP responses but had no effect on the control vs. facilitated differences.

Fig. 2C shows the effects of time shifting the control response from Fig. 1 by the average change in $t.9$ in 20 PPF experiments. The transformed waveform now

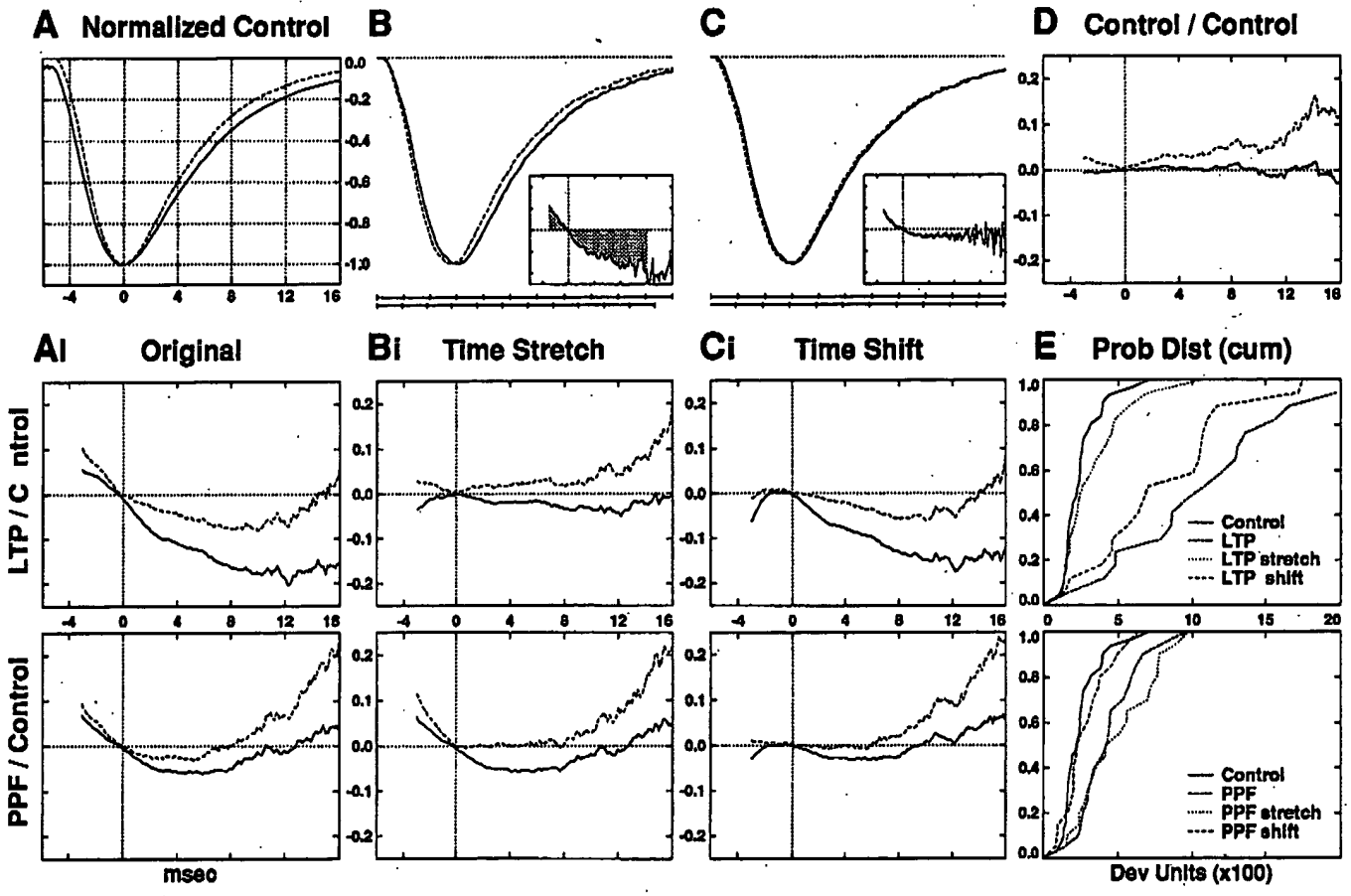

Fig. 2. Analysis of the waveform changes associated with LTP and PPF and of the effectiveness of the time translation and dilation transformations, based on the normalized subtraction and time-course deviation procedure. A: normalized control field EPSP (mean solid, +S.D. dashed) for 31 experiments where each response was scaled to the same amplitude (−1 mV) and the time at peak amplitude was used as the zero time reference. The decay τ of the mean trace is 6.58 ms. Ai: normalized subtraction (mean solid, +S.D. dashed) for the 17 pairs of control-LTP experiments and the 20 pairs of control-PPF experiments used in the study (upper and lower row, respectively). B: time dilation (dashed) of the control response in Fig. 1 (solid) by −5.9%; the average percent decrease in the decay τ after LTP (see Table I). The time axes in the lower part of the panel illustrate the way in which the transformation can be regarded as re-scaling the time-course of the response. The inset shows the normalized subtraction trace when the stretched trace is regarded as the experimental response. The shaded region illustrates the area involved in the calculation of the time-course deviation for the interval [−3,12] ms; the deviation is 10.9×100. Bi: as in panel Ai where each experimental response was stretched by the observed percent change in the decay τ with respect to its associated control response before the normalized subtraction was performed. C: time translation (dashed) of the control response in Fig. 1 (solid) by −0.18 ms; the average observed change in $t.9$ with PPF (see Table I). The transformation is characterized by an horizontal translation of the response as indicated by the time axes in the lower part of the panel. The normalized subtraction trace when considering the shifted trace as the experimental response is shown in the inset; its time-course deviation is 2.9×100. Ci: as in panel Ai where each experimental response was shifted by the observed change in $t.9$ with respect to its associated control response before the normalized subtraction was performed. D: as in panel Ai for 31 pairs of control responses taken an average of 14 min apart during baseline recording conditions. E: time-course deviation cumulative (sample) probability distributions of the normalized subtraction traces of the control–control pairs in panel D, and of each of the conditions in panels Ai, Bi and Ci. An (x,y) coordinate in a trace indicates the percent y of cases observed to have a deviation error of x or less. All distributions proved significantly different from that of the control–control pairs ($P < 0.005$ Kolmogorov-Smirnov statistic) except for shifted PPF and stretched LTP ($P > 0.2$). The median of the deviation error for LTP and PPF was 10.3 and 4.2 (×100), respectively.

closely resembles the facilitated response (see Fig. 1), and the normalized subtraction trace (inset) is analogous to that of the mean for the PPF experiments (Fig. 2Ai). Fig. 2Ci summarizes the group results of applying the time shift to the LTP and PPF experiments. The change in the $t.9$ measure for each experiment was used as the parameter to shift the potentiated or facilitated response prior to normalized subtraction of its control waveform. As shown, time shifting eliminated most of the discrepancies between control and facilitated responses but did not substantially improve the match between pre- and post-LTP waveforms.

Statistical evaluation of the effectiveness of the above transformations was carried out by considering the area between the normalized subtraction trace and the zero amplitude trace (illustrated by the shaded area in the inset to panel B in Fig. 2), normalized by the length of the relevant time period, as an error index. This corresponds to the notion of average percent error (which we have chosen to express as 'deviation error') in the time-course between the control and experimental traces. The time-course deviation was obtained for each of the 31 pairs of control–control responses used for panel 2D, and its distribution assumed as representative of the variability inherent in our experimental conditions. The same procedure was used to obtain the distributions of the time-course deviations for LTP and PPF, both before and after applying each of the above time transformations. The results obtained are presented in panel E (Fig. 2) as cumulative (sample) probability distributions. Comparison of the control–control deviation distribution versus those for PPF and LTP with the Kolmogorov–Smirnov statistic[13] to test the hypothesis that both were drawn from the same distribution proved negative and highly significant ($P < 0.005$) in all cases except for stretched LTP and shifted PPF ($P > 0.2$). The deviation distributions for LTP vs. PPF also proved to be significantly different ($P < 0.001$). These results do not depend on the use of the normalized subtraction procedure as the same outcome, both qualitative and quantitative, is obtained with the use of non-normalized subtraction (not shown). Based on the time-course deviation index, the above results indicate that: (i) the waveforms of facilitated and potentiated responses are significantly different from each other and from that of their associated control traces; (ii) the time stretch transformation applied to the LTP, but not the PPF, trace causes it to be statistically indistinguishable from its associated control response; and (iii) the time shift transformation applied to the PPF, but not the LTP, trace causes it to be statistically indistinguishable from its associated control response.

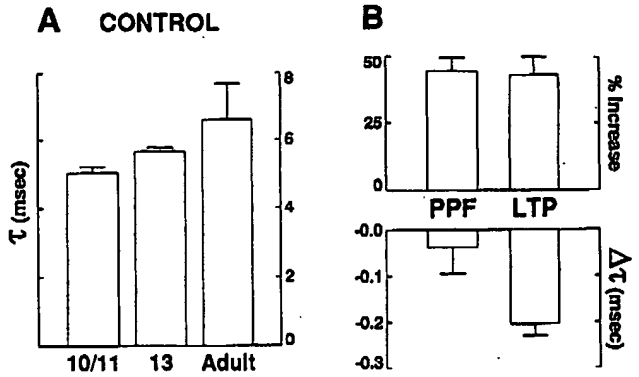

Fig. 3. Effects of PPF and LTP on the decay time constant of synaptic field potentials in neonatal slices. A: summary of the decay τ values of control responses ($\bar{x} + S.D.$) in adult ($n = 31$) post-natal day 13 ($n = 3$) and post-natal days 10 and 11 (P-10, $n = 2$; P-11, $n = 5$). The decay τ for the neonatal group was significantly smaller from that of the adult ($P < 0.001$ two-tailed t-test), and a negative correlation with age was observed within the neonatal group ($P < 0.05$ t-test, $r_s = -0.74$ Spearman's rank order correlation). B: summary of the results for paired pulse facilitation (PPF $n = 10$) and after the induction of LTP ($n = 8$) where 8 of the PPF experiments had the same control response as the LTP cases; pair-wise comparisons of the percent increase in amplitude (upper) and of the change in the decay τ (lower; $\bar{x} + S.E.M.$). The decay τ was not affected by PPF ($P > 0.1$) was significantly reduced after LTP ($P < 0.001$ two-tailed paired t-test), and the results for the two groups were statistically different from each other ($P < 0.05$ two-tailed t-test).

Preliminary modeling studies (Ambros-Ingerson et al. unpublished results) suggest that large (> 50%) reductions in the resistance of high impedance spine necks could in principle produce effects on the decay τ similar to those obtained with LTP. Accordingly, we tested for the effects of LTP on the decay τ using the same preparation as described above (IPSPs and postsynaptic spiking blocked) except that hippocampal slices were prepared from rats of post-natal days 10 to 13. It is known from anatomical work that CA1 dendrites are much simpler at these ages than in adults, and that most synapses are formed directly on the dendritic shaft or on primitive (sessile) spines[11,12]. Under these circumstances, spine neck resistance can be assumed to be of minimal significance. The decay τ of control responses ($n = 10$ experiments) was significantly smaller than that of the adult ($P < 0.001$ two-tailed t-test; Fig. 3A) and, within the group, negatively correlated with age ($r_s = -0.74$, Spearman's rank order correlation; $P < 0.05$ t-test), which is consistent with the much shorter dendritic arbors in the immature rats. The magnitude of LTP ($n = 8$ experiments) was slightly smaller than in the adults and in pair-wise comparisons (post- minus pre-LTP), was associated with a reduction in the decay τ (-0.20 ± 0.07 ms, $P < 0.001$ two-tailed paired t-test; Fig. 3B). Paired-pulse facilitation was tested in 10 cases and was similar in degree to the adult; no effects on the decay τ were found comparing

first and second responses (-0.04 ± 0.17 ms; Fig. 3B). PPF did, however, reduce $t.7$ by -0.17 ± 0.05 ms and $t.9$ by -0.21 ± 0.05 ms ($P < 0.001$ two-tailed paired t-test).

DISCUSSION

Several lines of evidence indicate that the decay τ of the hippocampal field EPSP (recorded in the absence of inhibitory currents), like the decay τ at neuromuscular junction[2,9] is closely related to the closing rate of post-synaptic receptor channels. The recorded mean and distribution of the decay τ's agrees with those for synaptic currents measured with whole-cell clamp[5]. The decay τ is unaffected by the degree of depolarization at the cell or at individual synapses, as shown by experiments using increased stimulation voltage to stimulate more synapses[1], paired-pulse facilitation to enhance release (see above and ref. 1) or kynurenic acid to partially block the pool of post-synaptic receptors (Xiao et al., unpublished results). This indicates that voltage-dependent currents do not contribute to the measured decay τ, as expected for an index determined by voltage-independent AMPA receptors[3,6] Finally, aniracetam, a drug that prolongs the mean open time of individual AMPA receptor channels[16], produces a corresponding increase in the decay τ of synaptic responses[1,16].

The decay τ thus provides a useful index for testing if LTP modifies the properties of AMPA receptors. The present studies confirm that LTP reduces the decay τ and show that the effect is also obtained in slices from neonatal hippocampus. Since the immature hippocampus has very simple spines and dendrites, the latter result argues against a contribution from spine biophysics to the LTP-induced changes, but is fully consistent with an explanation involving receptor modifications.

Alternative explanations, aside from a change in the kinetics of the receptor channel discussed below, cannot be completely ruled out by the present results alone. There are a number of constraints, however, that can be derived from our results that help in narrowing the range of possibilities. First, we emphasize that the LTP-associated waveform change is not likely related to alterations in the electrotonic properties of the cell as no changes were observed in the control pathway, indicating that all but synapse-specific properties remain unaltered. Second, it is not unlikely that a significant alteration in the geometry of the synaptic cleft would alter the time-course of the response by modifying the clearance rate of transmitter. However, in order to reduce the decay τ of the response the clearance rate must be increased (e.g. by broadening the cleft) which in turn is expected to reduce the size of the response. The converse argument also applies. Third, enhanced synchronization of stimulation of the target cells might occur after LTP induction, perhaps by increased synchronization of release, or alternatively by selective potentiation of the initially more synchronous axons stimulating the cell. A simple mathematical argument indicates that this consideration is not likely to alter the decay time of the response. In the simplest of cases, suppose the decay phase of the response has two components, with the same decay τ, but slightly displaced in time by t_o, hence $v(t) = A_1 e^{-t/\tau} + A_2 e^{-(t-t_o)/\tau}$. This expression is readily simplified to $v(t) = (A_1 + A_2 e^{-t_o/\tau}) e^{-t/\tau}$, which shows that the composite response exhibits the same decay τ as the individual responses, and that an alteration in synchronization (i.e. a change in t_o) is not likely to change the decay τ of the composite response.

Changes in the kinetics of gating channels (mean open time) underlying post-synaptic potentials have been reported[9], and are expected to affect not only the decay τ but also, and to a lesser degree, the early phases of the response. Confirmation of this point for the field EPSP has been obtained using aniracetam to prolong the mean open time of the AMPA receptor channel; i.e. the drug produced an increase in $t.7$ and $t.9$ smaller in size than its effect on the decay τ (Kolta et al., in preparation). As shown here, LTP caused a smaller reduction in the rise time than in the decay τ, and a significant positive correlation was obtained between the two indices. Indeed, the percent change in the decay τ substantially captured the overall waveform changes observed after potentiation as use of this single factor in the time-stretch transformation was sufficient to neutralize the highly significant LTP vs. control time-course deviations. Use of a previously described model of synaptic responses in CA1[15] shows that reductions in the mean open time of AMPA receptor channels would produce distortions of the waveform of the type found after LTP and that these can be corrected by stretching using the percent change in the measured decay τ as a parameter (Ambros-Ingerson et al., unpublished results). Together, these observations lead us to conclude that LTP reduces the mean open time of the AMPA receptor channel.

In addition to providing evidence that LTP modifies AMPA receptors, the above findings help to specify the nature of the modification. A reduction in mean open time will not increase synaptic currents and so presumably occurs as part of a general reconfiguration of the AMPA receptor that in toto enhances transmission. Thus, the present results predict that the receptor

can exist in a state in which its mean open time is reduced and its effective conductance and/or affinity increased.

Paired-pulse facilitation had the unexpected effect of reducing the time to reach 70% and 90% of peak amplitude. The early time-course changes are not particular to *t*.7 and *t*.9, as there is a continuous and positive deflection before the peak in the normalized subtraction traces (Fig. 2Ai). Sole information of the change in *t*.9 was sufficient to statistically annul the highly significant PPF-control time-course deviation, as shown by horizontally translating the PPF response (time-shift transformation) in the measure of the *t*.9 change (Fig. 2E). The absence of related changes in control experiments, where the second pulse was delivered hetero-synaptically, indicate that the observed effects are synapse-specific and not attributable to experimental artifacts. In all, the most parsimonious interpretation of the above results is that facilitated responses have an earlier onset with no alteration in waveform shape. It is not unlikely that an earlier onset is a reflection of the specific processes by which PPF increases the size of synaptic responses, perhaps an alteration in release kinetics. Interestingly, qualitative and, to some degree quantitative, effects of the kind we have described, have been reported in detailed modeling studies of the effects of paired stimulation on the time course of transmitter release[17].

Acknowledgements. Supported by the Air Force Office of Scientific Research Grant 89-0383. We thank Robert S. Zucker for his comments on an earlier version of this manuscript and Rafael Saavedra-Barrera and Chris Gall for helpful discussions.

REFERENCES

1 Ambros-Ingerson, J., Larson, J., Xiao, P. and Lynch, G., LTP changes the waveform of synaptic responses, *Synapse*, 9 (1991) 314–316.

2 Anderson, C.R. and Stevens, C.F., Voltage clamp analysis of acetylcholine produced end-plate current fluctuations at frog neuromuscular junction, *J. Physiol.*, 235 (1973) 655–691.

3 Ascher, P. and Nowak, L., Quisqualate- and kainate-activated channels in mouse central neurones in culture, *J. Physiol.*, 399 (1988) 227–245.

4 Bliss, T.V.P. and Lømo, T., Long lasting potentiation of synaptic transmission in the dentate area of the anaesthetized rabbit following stimulation of the perforant path, *J. Physiol.*, 232 (1973) 331–356.

5 Hestrin, S., Nicoll, R.A., Perkel, D.J. and Sah, P., Analysis of excitatory synaptic action in pyramidal cells using whole-cell recording from rat hippocampal slices, *J. Physiol.*, 422 (1990) 203–255.

6 Jahr, C.E. and Stevens, C.F., Glutamate activates multiple single channel conductances in hippocampal neurons, *Nature*, 325 (1987) 522–525.

7 Katz, B. and Miledi, R., The role of calcium in neuromuscular facilitation, *J. Physiol.*, 195 (1968) 481–492.

8 Larson, J., Wong, D. and Lynch, G., Patterned stimulation at the theta frequency is optimal for induction of long-term potentiation, *Brain Res.*, 368 (1986) 347–350.

9 Magleby, K.L. and Stevens, C.F., A quantitative description of end-plate currents, *J. Physiol.*, 223 (1972) 173–197.

10 Marquardt, D.W., An algorithm for least-squares estimation of non-linear parameters, *J. Soc. Indust. Appl. Math.*, 11 (1963) 431–441.

11 Pokorný, J. and Yamamoto, T., Postnatal ontogenesis of hippocampal CA1 area in rats. I. Development of dendritic arborization in pyramidal neurons, *Brain Res. Bull.*, 7 (1981) 113–120.

12 Pokorný, J. and Yamamoto, T., Postnatal ontogenesis of hippocampal CA1 area in rats. II. development of ultrastructure in stratum lacunosum moleculare, *Brain Res. Bull.*, 7 (1981) 121–130.

13 Press, W.H., Flannery, B.P., Teukolsky, S.A. and Vetterling, W.T, *Numerical Recipes in C*, Cambridge University Press, New York, 1989.

14 Royden, H.L., *Real Analysis*, MacMillan, New York, 1968.

15 Staubli, U., Ambros-Ingerson, J. and Lynch, G., Receptor changes and LTP: an analysis using aniracetam, a drug that modifies glutamate (AMPA) receptors, *Hippocampus*, 2 (1992) 49–58.

16 Tang, C.-M., Shi, Q.-Y., Katchman, A. and Lynch, G., Aniracetam modulates the time course of fast excitatory synaptic currents and glutamate channel kinetics, *Science*, 254 (1991) 288–290.

17 Yamada, W.M. and Zucker, R.S., Time course of transmitter release calculated from simulations of a calcium diffusion model, *Biophys. J.*, 61 (1992) 671–682.

18 Zucker, R.S., Changes in the statistics of transmitter release during facilitation, *J. Physiol.*, 229 (1973) 787–810.

Note added in proof

Recent modeling work indicates that a reduction in the channel's mean open time when coupled to a reduction in the mean time to open increases the effective conductance of the receptor in a release event [Ambros-Ingerson, J. and Lynch, G., Channel gating kinetics and synaptic efficacy: a hypothesis of LTP expression, *Proc. Natl. Acad. Sci. USA* (in press).